## Supplementary information

# Reversible Crystal Deformation of a Single-Crystal Host of Copper(II)1-Naphthoate—Pyrazine through Crystal Phase Transition Induced by Methanol Vapor Sorption

*Yuichi Takasaki and Satoshi Takamizawa**

Department of Nanosystem Science; Graduate School of Nanobioscience; Yokohama City University; 22-2 Seto; Kanazawa-ku, Yokohama, Kanagawa 236-0027; Japan

staka@yokohama-cu.ac.jp

## Table of contents

(a) Experimental information S2

(b) Crystallographic data and ortep drawings S3

(c) Connections of the crystal structures at the $\alpha/\beta$ interface S4-S5

## Other supplementary material

Video for crystal shape change of **1** observed under a microscope: Takamizawa_mov1.mov

(a) Experimental information

(Preparation of crystal)
Introducing pyrazine vapor (0.26 g, 3.3 mmol) into the methanol solution (60 mL) of copper(II) acetate monohydrate (0.102 g, 0.509 mmol) and 1-naphthoic acid (0.859 g, 4.99 mmol) gave blue green single crystals of **1** with a size of 100-500 μm in 30.9% yield (70.1 mg).

(X-ray single crystal diffraction analysis)
Single-crystal X-ray structural analysis of **1** was performed at 90 K and 293 K on a Bruker Smart APEX CCD area diffractometer (Bruker AXS K.K.) with a nitrogen-flow temperature controller using graphite-monochromated Mo $K\alpha$ radiation ($\lambda$ = 0.71073 Å). Empirical absorption corrections were applied using the SADABS program. The structure was solved by direct methods (SHELXS-97) and refined by full-matrix least-squares calculations on $F^2$ (SHELXL-97) using the SHELX-TL program package. Non-hydrogen atoms were refined anisotropically; hydrogen atoms were fixed at calculated positions by riding model approximation.

(Gas adsorption measurement)
$CO_2$ gas and MeOH vapor adsorption measurements were performed at 195 K and 293 K, respectively, on a Belsorp-max Measurement System (BEL JAPAN, Inc.) after drying the microcrystalline sample of **1** (13.80 mg for $CO_2$ gas adsorption and 24.70 mg for methanol vapor adsorption) at 373 K for 6 hours.

(b) Crystallographic data and ortep drawings

**Table S1.** Crystallographic data of **1**•0.93(MeOH) and **1**.

| Crystal phase | **1**•0.93(MeOH) (*β*) | **1** (*α*) | **1** (*α*) |
|---|---|---|---|
| Empirical formula | $C_{48.93}H_{35.72}Cu_2N_2O_{8.93}$ | $C_{48}H_{32}Cu_2N_2O_8$ | $C_{48}H_{32}Cu_2N_2O_8$ |
| Crystal size /mm$^3$ | 0.50 × 0.40 × 0.10 | 0.50×0.30×0.10 | 0.78×0.12×0.10 |
| M | 921.69 | 891.84 | 891.84 |
| Crystal system | Triclinic | Triclinic | Triclinic |
| Space group | *P*-1 | *P*-1 | *P*-1 |
| T /K | 90 | 90 | 293 |
| a /Å | 10.7482(17) | 10.4745(11) | 10.6065(8) |
| b /Å | 12.230(2) | 11.6064(12) | 11.6485(9) |
| c /Å | 16.366(3) | 17.0370(17) | 17.4513(14) |
| α /deg | 95.110(3) | 97.583(2) | 80.612(2) |
| β /deg | 96.968(3) | 104.918(2) | 75.2150(10) |
| γ /deg | 102.936(3) | 90.081(2) | 89.821(2) |
| V /Å$^3$ | 2066.2(3) | 1982.5(4) | 2055.1(3) |
| Z | 2 | 2 | 2 |
| $D_{calcd}$ / Mg m$^{-3}$ | 1.482 | 1.494 | 1.441 |
| μ(Mo Kα) / mm$^{-1}$ | 1.091 | 1.133 | 1.093 |
| Reflections collected | 10274 | 9616 | 10052 |
| Independent reflections ($R_{int}$) | 8394(0.0306) | 7440(0.0242) | 6592(0.0259) |
| Goodness of fit | 1.062 | 1.036 | 1.018 |
| $R_1$(I > 2σ (all data)) | 0.0580(0.0701) | 0.0429(0.0623) | 0.0509(0.0882) |
| $wR_2$(I > 2σ (all data)) | 0.1598(0.1699) | 0.1139(0.1264) | 0.1365(0.1625) |
| Largest diff. peak (hole) /eÅ$^3$ | 1.468(-1.016) | 0.952(-0.757) | 0.677(-0.596) |

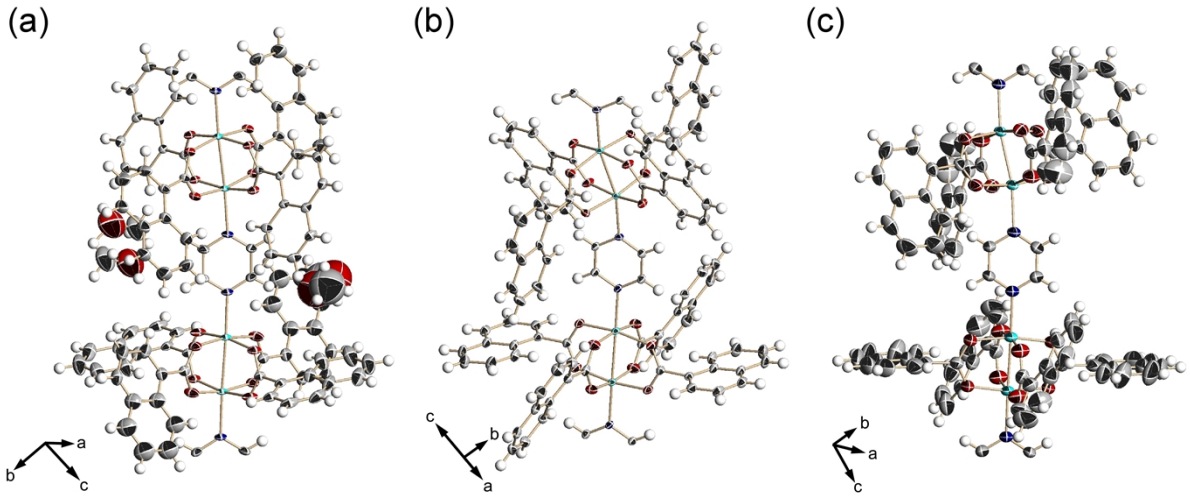


**Figure S1.** Molecular structures of (a) **1**•0.93(MeOH) at 90 K, (b) **1** at 90 K, and (c) **1** at 293 K as ortep view at 50% probability level for the each ellipsoid. The methanol molecules in **1**•0.93(MeOH) were disordered.

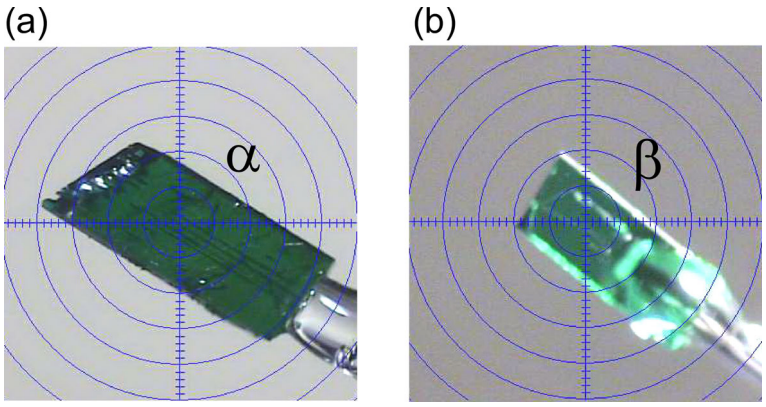


**Figure S2.** Single crystal of (a) **1** (α phase) and (b) **1**•0.93(MeOH) (β phase) used in single-crystal X-ray diffraction measurements at 90 K.

(c) Connections of the crystal structures at the $\alpha/\beta$ interface

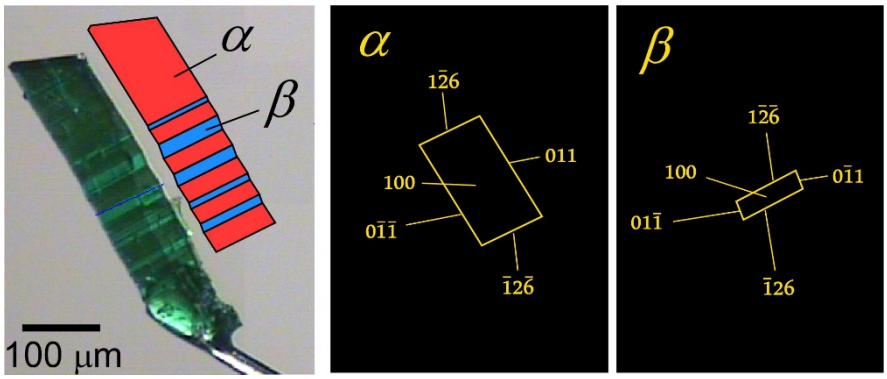


**Figure S3.** Crystal face indexing of **1** in $\alpha$-$\beta$ coexisting state at 293 K.

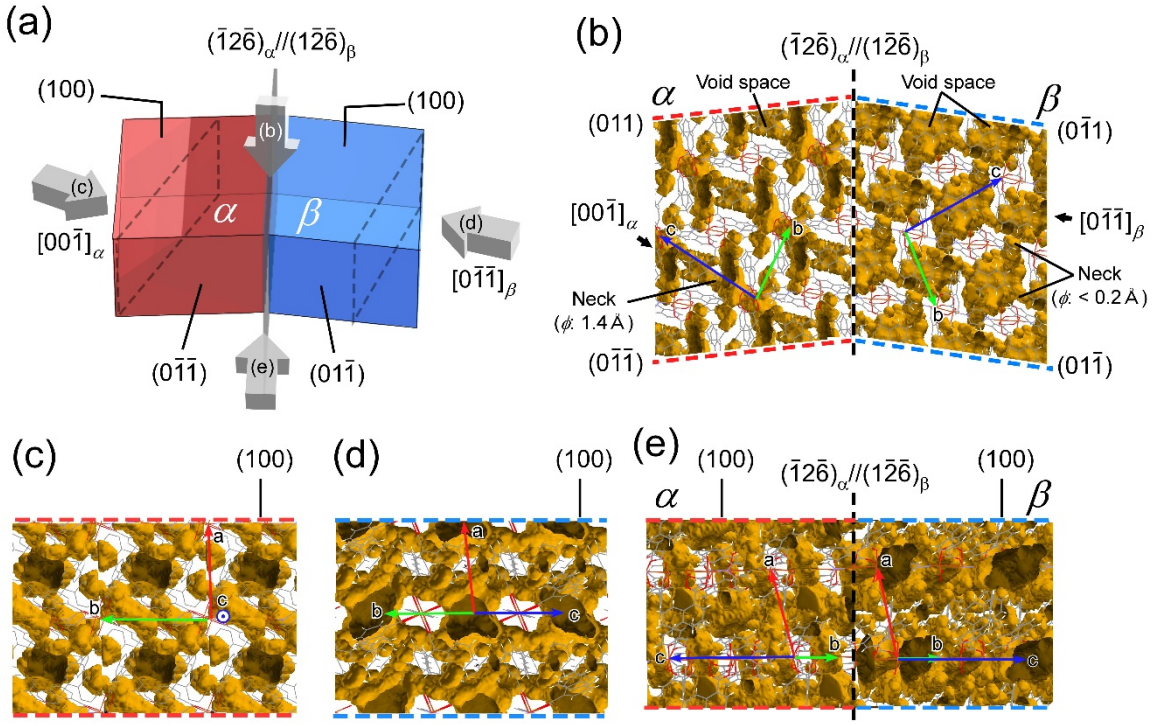


**Figure S4**. (a) Scheme for connections of $\alpha$ and $\beta$ phases on the interface. (b-e) Pore structures viewed along the four arrows illustrated in Fig. S4a. (b) Cross section on $(100)_{\alpha}$ and $(100)_{\beta}$. (c), (d) Cross sections indicated as dotted squares in Fig. S4a, which are oriented perpendicular to $[00\text{-}1]_{\alpha}$ and $[0\text{-}1\text{-}1]_{\beta}$, respectively. (e) Cross section perpendicular to $(100)_{\alpha}$, $(100)_{\beta}$, and $(\text{-}12\text{-}6)_{\alpha}//(1\text{-}2\text{-}6)_{\beta}$. Each void space in the $\alpha$ and $\beta$ phase was illustrated by Mercury software with a probe radius of 0.7 Å and grid spacing of 0.2 Å.